AD-A163 099 THEORY OF MULTICAVITY GYROKLYSTRON AMPLIFIER BASED ON A GREEN'S FUNCTION APPROACH(U) NAVAL RESEARCH LAB WASHINGTON DC A K GANGULY ET AL 29 NOV 85 NRL-8935 1/1

UNCLASSIFIED F/G 9/5 NL

END
FILMED
DTIC

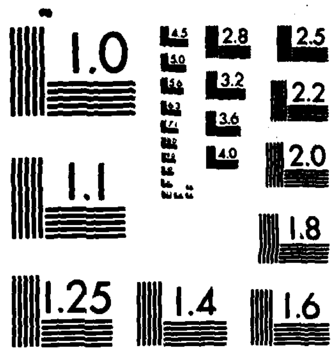

MICROCOPY RESOLUTION TEST CHART
NATIONAL BUREAU OF STANDARDS-1963-A

NAVAL RESEARCH LABORATORY
Washington, D.C.

Approved for public release; distribution unlimited.

AD-A163099

SECURITY CLASSIFICATION OF THIS PAGE

REPORT DOCUMENTATION PAGE

1a. REPORT SECURITY CLASSIFICATION UNCLASSIFIED	1b. RESTRICTIVE MARKINGS
2a. SECURITY CLASSIFICATION AUTHORITY	3. DISTRIBUTION/AVAILABILITY OF REPORT Approved for public release; distribution unlimited.
2b. DECLASSIFICATION/DOWNGRADING SCHEDULE	
4. PERFORMING ORGANIZATION REPORT NUMBER(S) NRL Report 8935	5. MONITORING ORGANIZATION REPORT NUMBER(S)
6a. NAME OF PERFORMING ORGANIZATION Naval Research Laboratory; 6b. OFFICE SYMBOL (If applicable) 6840	7a. NAME OF MONITORING ORGANIZATION
6c. ADDRESS (City, State, and ZIP Code) Washington, DC 20375-5000	7b. ADDRESS (City, State, and ZIP Code)
8a. NAME OF FUNDING/SPONSORING ORGANIZATION Space and Naval Warfare Systems Command; 8b. OFFICE SYMBOL (If applicable)	9. PROCUREMENT INSTRUMENT IDENTIFICATION NUMBER
8c. ADDRESS (City, State, and ZIP Code) Washington, DC 20363-5100	10. SOURCE OF FUNDING NUMBERS: PROGRAM ELEMENT NO. 62762N; PROJECT NO.; TASK NO. X562-584-100; WORK UNIT ACCESSION NO. DN020-179

11. TITLE (Include Security Classification)

Theory of Multicavity Gyroklystron Amplifier Based on a Green's Function Approach

12. PERSONAL AUTHOR(S)
Ganguly, A.K., Fliflet, A.W., and McCurdy, A.H.*

13a. TYPE OF REPORT	13b. TIME COVERED	14. DATE OF REPORT (Year, Month, Day)	15. PAGE COUNT
Final	FROM ______ TO ______	1985 November 29	18

16. SUPPLEMENTARY NOTATION

*Applied Physics Section, Yale University, New Haven, CT 06520

17. COSATI CODES			18. SUBJECT TERMS (Continue on reverse if necessary and identify by block number)
FIELD	GROUP	SUB-GROUP	Gyroklystron; Gyrotron; Cyclotron; Resonance

19. ABSTRACT (Continue on reverse if necessary and identify by block number)

This report presents an application of a self-consistent field theory for gyrotrons to a multicavity gyroklystron configuration. The coupled radio frequency ~~(RF)~~ field equation and the Lorentz equations are solved in the slow-time scale formulation by using a Green's function technique to satisfy appropriate boundary conditions. An analytical expression for the small signal gain is obtained by successive approximation. The theory has been developed for cylindrical TE_{mnl} mode as well as rectangular TE_{101} mode. The theory is applied to calculate the small signal performance characteristics of a three-cavity configuration operating with rectangular TE_{101} mode. Keywords:

20. DISTRIBUTION/AVAILABILITY OF ABSTRACT ☐ UNCLASSIFIED/UNLIMITED ☒ SAME AS RPT ☐ DTIC USERS	21. ABSTRACT SECURITY CLASSIFICATION UNCLASSIFIED
22a. NAME OF RESPONSIBLE INDIVIDUAL A.K. Ganguly	22b. TELEPHONE (Include Area Code) (202) 767-3382; 22c. OFFICE SYMBOL 6840

DD FORM 1473, 84 MAR — 83 APR edition may be used until exhausted. All other editions are obsolete.

SECURITY CLASSIFICATION OF THIS PAGE

CONTENTS

THEORY OF MULTICAVITY GYROKLYSTRON AMPLIFIER BASED ON A GREEN'S FUNCTION APPROACH

INTRODUCTION

Gyroklystron amplifiers show great promise as high-power and high-gain devices in the microwave and millimeter wavelengths. Jory et al. [1] performed the first gyroklystron amplifier experiment in a two-cavity configuration with cylindrical $TE^{\circ}_{011}/TE^{\circ}_{021}$ modes. Recently, Bollen et al. [2] have performed a three-cavity gyroklystron amplifier experiment operating with rectangular TE°_{101} mode at 4.2 GHz. They achieved an output power of 54 kW with 16% efficiency and 0.2% bandwidth. To achieve higher gain and moderate bandwidth, a multicavity configuration with staggered tuning will be necessary as in conventional klystrons. The design of such a configuration requires the optimization of many parameters. The large signal analysis and numerical codes [3-5] developed previously for two-cavity gyroklystrons can be extended to the multicavity configuration, but the procedure would require extremely large computation time. Moreover, the bandwidth and the effect of staggered tuning could not be calculated since the radio frequency (RF) fields are not determined self-consistently. Therefore, it is necessary to develop an analytical linear theory for multicavity gyroklystrons. The linear theory will be applicable to the prebunching cavities where RF field is small, and these results may be used as an input for large signal calculation in the power extraction cavity to obtain saturation gain and efficiency. Symons and Jory [6] developed a small signal theory for the two-cavity gyroklystron by using a sinusoidal RF profile and obtained equivalent circuit parameters. Caplan [7] outlined a small signal self-consistent theory of gyroklystron amplifier based on Maxwell-Vlasov theory. In this report, we develop a self-consistent theory of the multicavity gyroklystron amplifier in which the electron motion is represented by the generalized pendulum equation [8,9]. The derivation of these equations [10] are outlined in the next section. These equations are solved in the third section for the multicavity gyroklystron configuration by using a Green's function approach to satisfy appropriate RF field boundary conditions. Small signal results are then obtained by the method of successive approximation. Effects of axial beam velocity spread are also included. In the fourth section we calculate the small signal performance characteristics of the three-cavity gyroklystron amplifier configuration used by Bollen et al. [2].

SELF-CONSISTENT EQUATIONS FOR GYROTRONS

Figure 1 illustrates the multicavity gyroklystron amplifier under study. The cavities, separated by drift regions, are placed in a uniform magnetic field $\vec{B}_0$ applied parallel to the axes of the cavities (z-axis). Let $r_{w,j}$ and L_j denote the radius and the length of the jth cavity; d_j is the length of the jth drift region. The entrance of the jth cavity is at

$$z = z_j = \sum_{i=1}^{j-1}(L_i + d_i)\,.$$

An input RF signal and a monoenergetic beam of electrons are injected from the left into the first cavity. The electrons follow helical trajectories due to the strong uniform magnetic field and experience perturbing RF fields in the cavities. It is assumed that the RF fields are completely cut off in the drift regions. Space charge effects are also neglected.

Manuscript approved July 22, 1985.

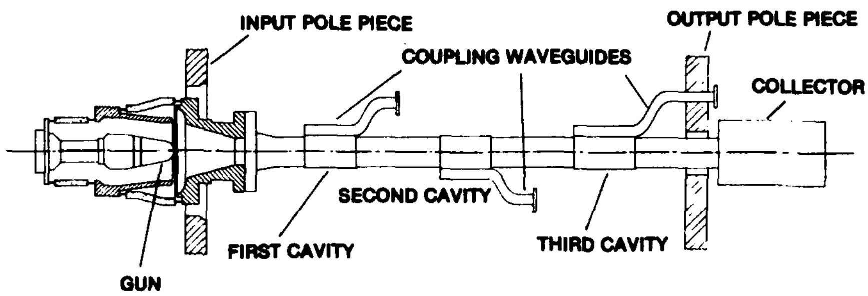

Fig. 1 — A three-cavity gyroklystron

Consider the beam interaction with the electric field of a TE-type circular waveguide mode. Under most gyroklystron operating conditions (electron velocity v_e much less than phase velocity v_p), the electron beam interaction with RF magnetic field may be neglected. For propagation of a single TE_{mn} mode, the electric field is given by

$$\vec{E}_t = \mathrm{Re}[C_{mn}\{k_{mn}J'_m(k_{mn}r)\hat{e}_\theta + (im/r)J_m(k_{mn}r)\hat{e}_r\}F(z)e^{i(\omega t - m\theta)}], \tag{1}$$

where ω is the wave frequency, J_m is a Bessel function of order m, the prime denotes differentiation, and k_{mn} is the transverse wave number. The normalization constant is given by

$$C_{mn} = [\{\pi(x_{mn}^2 - m^2)\}^{1/2}J_m(x_{mn})]^{-1}, \tag{2}$$

and

$$k_{mn} = x_{mn}/r_w, \tag{3}$$

where x_{mn} is the nth zero of J'_m. The axial dependence of the RF fields in the cavities is given by the complex profile function

$$F(z) = |F(z)|e^{-i\xi(z)}. \tag{4}$$

$|F(z)|$ and $d\xi(z)/dz$ are assumed to be slowly varying functions of z such that $\lambda_c \frac{d|F|}{dz} < |F|$ and similarly for the phase. Here $\lambda_c = 2\pi\, v_z/\omega$.

In uniform external magnetic field, the axial momentum (p_z) of the electrons remains constant if the RF magnetic field is neglected. For small values of $\gamma = [1 + p_\perp^2 + p_z^2]^{1/2}$, we will assume that v_z is approximately constant. For operation near cyclotron resonance (i.e., $\omega - \frac{s\Omega_0}{\gamma} << \omega$), it is convenient to write the transverse components (p_x, p_y) of the electrons in the following form:

$$p_x = -p_\perp(t)\sin\{\Omega(t)\tau + \phi(t)\}, \tag{5}$$

$$p_y = p_\perp(t)\cos\{\Omega(t)\tau + \phi(t)\}, \tag{6}$$

where

$$\Omega = |e|B_0/m_0\gamma = \Omega_0/\gamma, \tag{7}$$

$$\tau = t - t_0, \tag{8}$$

and Ω, $p_\perp$, and ϕ are slow-time scale variables; t_0 is the time the electrons enter the interaction region. Under these approximations, it has been shown [10,11] that the Lorentz force equations for the electrons can be expressed approximately in the following form in terms of two slow-time scale variables $p_\perp$ and the phase angle $\Lambda = \omega t - \Omega\tau - \phi$:

$$\frac{dp_\perp}{dt} = -|e|C_{ml}k_{ml}J_{m-s}(k_{ml}r_0)\, J'_s(k_{ml}r_L)|F|\cos\Psi, \tag{9}$$

$$p_\perp \frac{d\Lambda}{dt} = |e| C_{ml} k_{ml} J_{m-s}(k_{ml} r_0) \frac{s J_s(k_{ml} r_L)}{k_{ml} r_L} |F| \sin \Psi + (\omega - s\Omega) p_\perp, \tag{10}$$

where s is the cyclotron harmonic number and r_0 and r_L are the guiding center radius and the Larmor radius. The phase Ψ in Eqs. (9) and (10) is given by

$$\begin{aligned}\Psi &= \left(\omega - \frac{s\Omega_0}{\gamma}\right)(t - t_0) + \omega t_0 - \xi - \phi - (m - s)\theta_0 \\ &= \Lambda - \xi - (m - s)\theta_0,\end{aligned} \tag{11}$$

where θ_0 is the polar angle of the guiding center.

The wave equation for the electric field profile function $F(z)$ may be written as [10]

$$\begin{aligned}&\left[\frac{d^2}{dz^2} + \frac{\omega^2}{c^2}\left(1 - \frac{i}{Q}\right) - k_{mn}^2\right] F \\ &= -i \frac{\mu \omega I_0}{m_0 \gamma v_{\|,av}} C_{mn} k_{mn} J_{m-s}(k_{mn} r_0) < p_\perp J_{s-1}(k_{mn} r_L) e^{-is\Lambda} >,\end{aligned} \tag{12}$$

where $I_0 = n_0 |e| v_{\|,av}$ is the beam current, and Q represents losses from the cavity. In Eq. (12), $<0>$ denotes an average over initial electron phase $\Lambda_0 = \omega t_0$, the initial guiding center distribution and initial electron velocity distribution function $f(\overline{v})$:

$$<0> = \int f(\overline{v}) d\overline{v} \frac{1}{(2\pi)^2} \int_0^{2\pi} \int_0^{2\pi} 0 \, d\Lambda_0 d\theta_0.$$

For a "cold" beam, $<0>$ involves an average only over initial phase and guiding center position. For this case $v_{\|,av} = v_\|$.

For fundamental cyclotron harmonic operation ($s = 1$), Eqs. (9) to (12) can be further simplified by noting that $k_{mn} r_L << 1$. Hence $J_1'(k_{mn} r_L)$ and $J_1(k_{mn} r_L)/k_{mn} r_L$ can be replaced by the leading term of the small argument expansion of the Bessel function; i.e.,

$$J_1'(k_{mn} r_L) \cong J_1(k_{mn} r_L)/k_{mn} r_L \cong 1/2.$$

It is now convenient to introduce a complex slow-time scale transverse momentum given by

$$p = p_\perp e^{-i\Lambda}. \tag{13}$$

Equations (9), (10), and (12) become

$$\begin{aligned}&\frac{dp}{dz} + \frac{i}{v_\|}\left(\omega - \frac{\Omega_0}{\gamma}\right) p \\ &= -\frac{|e| C_{mn} k_{mn}}{2 v_\|} J_{m-1}(k_{mn} r_0) F e^{-i(m-1)\theta_0},\end{aligned} \tag{14}$$

and

$$\begin{aligned}&\left[\frac{d^2}{dz^2} + \left\{\frac{\omega^2}{c^2}\left(i - \frac{i}{Q}\right) - k_{mn}^2\right\}\right] F \\ &= -\frac{i \mu_0 \omega I_0}{\gamma m_0 v_{\|,av}} C_{mn} k_{mn} J_{m-1}(k_{mn} r_0) < p e^{i(m-1)\theta_0} >.\end{aligned} \tag{15}$$

In Eq. (14), we have used the relation $\frac{d}{dt} = v_z \frac{d}{dz}$. The generality of Eqs. (14) and (15) can be increased by a normalization scheme in which the wavelength λ_0 of the radiation is an arbitrary

number. For finite bandwidth operation, λ_0 will refer to the center frequency of the band. The normalization scheme can be achieved as follows (the normalized quantities are denoted by a bar):

(a) length normalized to $\lambda_0(\bar{z} = z/\lambda_0)$

(b) velocity normalized to $c\,(\beta = v/c)$

(c) frequency normalized to $\dfrac{c}{\lambda_0}\left(\bar{\omega} = \dfrac{\omega\lambda_0}{c}\right)$

(d) electric and magnetic fields normalized to

$$(\bar{E} = eE\lambda_0/m_0c^2,\ \bar{B}_0 = eB_0\lambda_0/m_0c).$$

Other quantities such as k_{mn}, p, t, and F are normalized consistently to $\bar{k}_{mn} = k_{mn}\lambda_0$, $\bar{p} = p/m_0c$, $\bar{t} = tc/\lambda_0$, and $\bar{F} = eF/m_0c^2$. After these procedures, Eqs. (14) and (15) become

$$\frac{d\bar{p}}{d\bar{z}} + \frac{i}{\beta_{\parallel}}\left(\bar{\omega} - \frac{\Omega_0}{\gamma}\right)\bar{p} = -\frac{\beta_{\parallel,av}}{\beta_{\parallel}}\bar{E}, \tag{16}$$

$$\left(\frac{d^2}{d\bar{z}^2} + \bar{k}_z^2\right)\bar{E} = -i\bar{I}_0<\bar{p}>, \tag{17}$$

where

$$\bar{k}_z = \left[\frac{\omega^2}{c^2}\left(1 - \frac{i}{Q}\right) - k_{mn}^2\right]^{1/2}\lambda_0,$$

$$\bar{E} = \frac{1}{2}\cdot\frac{C_{mn}}{\beta_{\parallel,av}}\,\bar{k}_{mn}J_{m-1}(\bar{k}_{mn}\bar{r}_0)\bar{F}e^{-i(m-1)\theta_0}, \tag{18}$$

and

$$\bar{I}_0 = \frac{1}{2\pi}\cdot\frac{eI_0}{\epsilon_0m_0\gamma c^3}\cdot\frac{\bar{k}_{mn}^2\bar{\omega}}{\beta_{\parallel,av}^2}\cdot\frac{J_{m-1}^2(\bar{k}_{mn}\bar{r}_0)}{(x_{mn}^2 - m^2)J_m^2(x_{mn})}. \tag{19}$$

Equations (16) and (17) constitute a set of nonlinear coupled equations for the gyrotron. In the next section we give an analytical solution of these equations in the linear approximation.

GREEN'S FUNCTION APPROACH AND LINEAR THEORY

We solve Eqs. (16) and (17) for a "cold" beam where $\beta_{\parallel,av} = \beta_{\parallel}$. At the end of this section we point out the modification necessary to consider axial velocity spread of the beam.

The general solution of Eqs. (16) and (17) may be written as

$$\bar{p}(\bar{z}) = [\bar{p}(\bar{z}_j) - \int_{\bar{z}_j}^{\bar{z}}\bar{E}(\bar{z}')e^{i\int_{\bar{z}_j}^{\bar{z}'}\Delta(\bar{z}'')d\bar{z}''}d\bar{z}']e^{-i\int_{\bar{z}_j}^{\bar{z}}\Delta(\bar{z}')d\bar{z}'} \tag{20}$$

and

$$\begin{aligned}\bar{E}(\bar{z}) = -i\bar{I}_0\int_0^{\bar{L}_j}G(\bar{z},\bar{z}')<\bar{p}(\bar{z}')>d\bar{z}'\\ + A_j\sin\bar{k}_{z,j}(\bar{z} - \bar{z}_j - \bar{L}_j),\end{aligned} \tag{21}$$

where

$$\bar{z}_j = \sum_{i=1}^{j-1}(\bar{L}_i + \bar{d}_i),$$

$$\bar{k}_{z,j} = \left[\frac{\omega^2}{c^2}\left(1 - \frac{i}{Q_j}\right) - \left(\frac{x_{mn}}{r_{w,j}}\right)^2\right]^{1/2}\lambda_0,$$

and the detuning parameter

$$\Delta(\bar{z}) = \frac{1}{\beta_{\parallel}}\left\{\bar{\omega} - \frac{\bar{\Omega}_0}{\gamma(z)}\right\}. \tag{22}$$

In Eq. (21) the first term is the particular integral giving the contribution to the field due to the perturbed current density, and the second term is the homogeneous solution. $G(z, z')$ is the Green's function and should be chosen to satisfy the correct boundary conditions. If we assume that $\bar{E}(\bar{z})$ vanishes at both $\bar{z} = \bar{z}_j$ and $\bar{z} = \bar{z}_j + \bar{L}_j$, then $G(\bar{z}, \bar{z}')$ is represented by

$$G(\bar{z}, \bar{z}') = \frac{1}{\bar{k}_{z,j} \sin \bar{k}_{z,j}\bar{L}_j}\begin{cases} \sin \bar{k}_{z,j}\bar{z} \sin \bar{k}_{z,j}(\bar{z}' - \bar{L}_j), \sin \bar{z} < \bar{z}' \\ \sin \bar{k}_{z,j}\bar{z}' \sin \bar{k}_{z,j}(\bar{z} - \bar{L}_j), \ \bar{z}' < z \end{cases}. \tag{23}$$

This form of $G(\bar{z}, \bar{z}')$ applies to all the cavities except the first and the last ones. In those two cavities, boundary conditions corresponding to the incoming and outgoing waves might be included. In this report we assume that Eq. (23) applies to the last cavity also. In the first cavity the input signal produces energy modulation on the electron beam. If the beam current is not too high and the cavity is short, then the change in energy of the electrons in the first cavity is small and the input signal is perturbed only slightly by the electron beam. Under these circumstances, the electric field in the cavity is well represented by the homogeneous solution

$$\bar{E}(\bar{z}) = \bar{E}_{01} \sin \bar{k}_{z,1}(\bar{L}_1 - \bar{z}), \tag{24}$$

where $\bar{E}_{01}$ is related to the input power incident at $z = 0$. In all other cavities, the RF field is induced by the bunched beam, and the homogeneous part of the solution in Eq. (21) will be neglected. We have already mentioned that $\bar{E}(z) = 0$ in the drift regions, i.e., $\bar{z}_j + \bar{L}_j < \bar{z} < \bar{z}_j + \bar{L}_j + \bar{d}_j$.

In the small signal regime, the two integral Eqs. (20) and (21) may be solved by the method of successive approximation where $\bar{E}_{01}$ will be considered a small quantity. The initial condition are chosen to be

$$\begin{aligned} \bar{p}(0) &= \bar{p}_{\perp 0}e^{-i\phi_0}, \quad o < \phi_0 < 2\pi, \\ \bar{E}(0) &= \bar{E}_{01} \sin \bar{k}_{z,1}\bar{L}_1. \end{aligned} \tag{25}$$

By retaining terms up to first order in $\bar{E}_{01}$, we find from Eqs. (20) and (24) that the transverse momentum at the end of the first cavity ($\bar{z} = \bar{L}_1$) of an electron with initial phase ϕ_0 is given by

$$\bar{p}(\bar{L}_1, \phi_0) = \bar{p}_{\perp 0}\left\{1 - \frac{\bar{E}_{01}}{\bar{p}_{\perp 0}} R_1 e^{i\phi_0}\right\} e^{-i(\phi_0 + \chi(\bar{L}_1))}, \tag{26}$$

where

$$\begin{aligned} R_1 &= \int_0^{\bar{L}_1} \sin \bar{k}_{z,1}(\bar{L}_1 - \bar{z}')\, e^{i\Delta_0\bar{z}'} d\bar{z}' \\ &= \frac{\bar{k}_{z,1}\{\cos(\bar{k}_{z,1}\bar{L}_1) - \cos(\Delta_0\bar{L}_1)\} + i(\Delta_0 \sin \bar{k}_{z,1}\bar{L}_1 - \bar{k}_{z,1} \sin \Delta_0\bar{L}_1)}{\Delta_0^2 - \bar{k}_{z,1}^2}, \end{aligned} \tag{27}$$

$$\Delta_0 = \frac{1}{\beta_{\parallel}}\left\{\bar{\omega} - \frac{\bar{\Omega}_0}{\gamma(0)}\right\}, \tag{28}$$

$$\chi(\bar{z}) = \int_0^{\bar{z}} \Delta(\bar{z}')d\bar{z}' \cong \Delta_0\bar{z} + \frac{\Omega_0}{\gamma_0\beta_{\parallel}} \int_0^{z} \frac{\delta\gamma}{\gamma} d\bar{z}', \tag{29}$$

$$\frac{\delta\gamma}{\gamma} \cong \frac{|\bar{p}(\bar{z})|^2 - p_{\perp 0}^2}{2\gamma_0^2} \cong \frac{|\bar{p}(\bar{z}_j)|^2 - \bar{p}_{\perp 0}^2}{2\gamma_0^2} - \mathrm{Re}\,\frac{\bar{p}^*(\bar{z}_j)}{\gamma_0^2}\int_{\bar{z}_j}^{\bar{z}} \bar{E}(\bar{z}')e^{i\Delta_0\bar{z}'}\,d\bar{z}', \tag{30}$$

$$\bar{k}_{z,j} = \left\{\bar{\omega}^2\left(1 - \frac{i}{Q_j}\right) - \frac{x_{mn}^2}{\bar{r}_{w,j}^2}\right\}^{1/2}. \tag{31}$$

From Eqs. (24), (29), and (30), we have

$$\chi(\bar{L}_1) \equiv \chi_1$$
$$= \Delta_0\bar{L}_1 - \frac{\bar{p}_{\perp 0}\bar{\Omega}_0}{\gamma_0^3\beta_{11}}\,\mathrm{Re}\{\bar{E}_{01}T_1e^{i\phi_0}\}, \tag{32}$$

where

$$T_1 = \{(\Delta_0^2 - \bar{k}_{z,1}^2)\bar{k}_{z,1}\bar{L}_1\cos\bar{k}_{z,1}\bar{L}_1 + (\Delta_0^2 + \bar{k}_{z,1}^2)\sin\bar{k}_{z,1}\bar{L}_1$$
$$- 2\Delta_0\bar{k}_{z,1}\sin\Delta_0\bar{L}_1\}/(\Delta_0^2 - \bar{k}_{z,1}^2)^2$$
$$+ i\{(\Delta_0^2 - \bar{k}_{z,1}^2)\,\Delta_0\bar{L}_1\sin\bar{k}_{z,1}\bar{L}_1 + 2\Delta_0\bar{k}_{z,1}(\cos\Delta_0\bar{L}_1 - \cos\bar{k}_{z,1}\bar{L}_1)\}/(\Delta_0^2 - \bar{k}_{z,1}^2)^2. \tag{33}$$

The change in γ in the first cavity for an electron with initial phase ϕ_0 is given to first order in E_{01} by

$$\frac{\Delta\gamma}{\gamma_0} \cong \frac{|\bar{p}(\bar{L}_1)|^2 - \bar{p}_{\perp 0}^2}{2\gamma_0^2} = -\frac{\bar{p}_{\perp 0}}{\gamma_0^2}\,\mathrm{Re}\{\bar{E}_{01}R_1e^{i\phi_0}\}. \tag{34}$$

Since we have assumed that $\bar{E}(\bar{z}) = 0$ in the drift regions, we find from Eqs. (34) and (30) that the transverse momentum $\bar{p}$ at the end of the first drift region is given by

$$\bar{p}(\bar{L}_1 + \bar{d}_1, \phi_0) = \bar{p}_{\perp 0}\left\{1 - \frac{\bar{E}_{01}R_1e^{i\phi_0}}{\bar{p}_{\perp 0}}\right\} e^{-i(\bar{L}_1+\bar{d}_1)\Delta_0}\, e^{-i[\phi_0 - X_{11}\cos\phi_{01}']}, \tag{35}$$

where

$$X_{11} = \frac{\bar{p}_{\perp 0}\bar{\Omega}_0}{\gamma_0^3\beta_{\parallel}}|\bar{E}_{01}(T_1 + R_1\bar{d}_1)|, \tag{36}$$

$$\phi_{01}' = \phi_0 + arg(T_1 + R_1\bar{d}_1) + arg(\bar{E}_{01}) = \phi_0 + \hat{\delta}_1. \tag{37}$$

By averaging Eq. (35) over the initial phase ϕ_0, we get

$$<\bar{p}(\bar{L}_1 + \bar{d}_1)> = ip_{\perp 0}\left\{J_1(X_{11}) + i\frac{\bar{E}_{01}R_1e^{-i\hat{\delta}_1}}{\bar{p}_{\perp_0}}J_0(X_{11})\right\} e^{-i[(L_1+d_1)\Delta_0 - \hat{\delta}_1]}. \tag{38}$$

In writing Eq. (38) we have used the relations

$$\frac{1}{2\pi}\int_0^{2\pi} e^{-i[\theta - x\cos\theta]}\,d\theta = iJ_1(x),$$
$$\frac{1}{2\pi}\int_0^{2\pi} e^{ix\cos\theta}\,d\theta = J_0(x).$$

The presence of the term $X_{11}\cos(\phi_0 + \delta_1)$ in the phase in Eq. (35) shows that the electrons are bunched although initially they have a uniform phase distribution. X_{11} may be interpreted as the "bunching parameter" in the first stage of the amplifier. If the bunching in the first cavity is

neglected and k_z is set equal to π/L, then the bunching parameters X_{11} given by Eq. (36) reduces to the expression given by Symons and Jory [6] for the two-cavity gyroklystron. Although $\bar{E}_{01}$ is small, we do not make the small argument expansion for $J_0(X_{11})$ and $J_1(X_{11})$ with a view toward the investigation of the effects of nonlinear inertial bunching in long drift regions. $\bar{p}(\bar{L}_1 + \bar{d}_1, \phi_0)$ given by Eq. (35) will serve as initial condition for the calculation of $\bar{p}$ and $\bar{E}$ in the second cavity.

In the small signal regime, the phase-averaged momentum ($<p>$) changes by a small amount in each cavity and the phase space bunching occurs mainly in the drift regions. Therefore in Eq. (21), we may make the approximation that $<\bar{p}>$ is constant and replace it by its value at the entrance of the cavity, i.e., at $\bar{z} = \bar{z}_j = \sum_{i=1}^{j-1} (\bar{L}_i + \bar{d}_i)$. With this approximation and neglecting the homogeneous solution ($A_j = 0$) in Eq. (21), we can solve for $\bar{p}(\bar{z})$ and $\bar{E}(\bar{z})$ by the method of successive approximation in all cavities $j \geqslant 2$. After lengthy algebra, the following equations are obtained correct to first order in $\bar{E}_{01}$. The transverse momentum of the electron at the end of the jth stage is

$$\bar{p}(\bar{z}_{j+1}, \phi_0) = \bar{p}_{\perp 0}\left\{1 - \sum_{l=1}^{j} \frac{\bar{E}_{0l} R_l e^{i\psi_l}}{\bar{p}_{\perp 0}}\right\} e^{-i[\psi_{j+1} + \bar{z}_{j+1}\Delta_0 - \hat{\delta}_j]}, \tag{39}$$

and the electric field profile $\bar{E}(\bar{z})$ in the jth cavity is

$$\bar{E}(\bar{z}) = \bar{E}_{0j}\, e^{-i(\Delta_0 \bar{z}_j - \hat{\delta}_{j-1})} \int_0^{\bar{L}_j} G(z,z')\, dz'. \tag{40}$$

The complex quantity E_{0l} for $l \geqslant 2$ is defined by

$$\begin{aligned} \bar{E}_{0l} &= -i\bar{I}_0 <\bar{p}(\bar{z}_l)>\, e^{i[\bar{z}_l \Delta_0 - \hat{\delta}_{l-1}]} \\ &= \bar{I}_0 \bar{p}_{\perp 0}\Bigg[J_1(\hat{X}_{l-1}) + i\frac{\bar{E}_{01} R_1}{\bar{p}_{\perp 0}} J_0(\hat{X}_{l-1}) e^{-i\hat{\delta}_{l-1}} \\ &\qquad + i(1 - \delta_{l,2}) \sum_{l'=1}^{l-2} J_0(\hat{X}_{l',l-1}) \frac{\bar{E}_{0l'} R_{l'}}{\bar{p}_{\perp 0}} e^{-i(\hat{\delta}_{l-1} - \hat{\delta}_{l'})}\Bigg], \end{aligned} \tag{41}$$

where

$$\begin{aligned} \delta_{l,2} &= 1 \text{ if } l = 2 \\ &= 0 \text{ if } l \neq 2 \end{aligned}$$

$$\hat{X}_l e^{i\hat{\delta}_l} = \sum_{j=1}^{l} \sum_{j'=j}^{l} X_{jj'}\, e^{i\xi_{jj'}}, \tag{42}$$

$$X_{jj} = \frac{\bar{\Omega}_0 \bar{p}_{\perp 0}}{\beta_{\parallel} \gamma_0^3} |\bar{E}_{0j}(T_j + R_j \bar{d}_j)|, \tag{43}$$

$$X_{ij} = \frac{\bar{\Omega}_0 \bar{p}_{\perp 0}}{\beta_{\parallel} \gamma^3} |\bar{E}_{0i} R_i (\bar{L}_j + \bar{d}_j)|, \qquad i < j \tag{44}$$

$$\hat{X}_{ij} = |\hat{X}_j e^{i\hat{\delta}_j} - \hat{X}_i e^{i\hat{\delta}_i}|, \qquad i < j \tag{45}$$

and

$$\begin{aligned} \xi_{11} &= arg(\bar{E}_{01}) + arg(T_1 + R_1 \bar{d}_1), \\ \xi_{jj} &= arg(\bar{E}_{0j}) + arg(T_j + R_j \bar{d}_j) + \hat{\delta}_{j-1}, \qquad j \geqslant 2 \end{aligned} \tag{46}$$

$$\xi_{ij} = arg(\bar{E}_{0i}) + arg(R_j), \qquad j \geqslant 2$$

$$\hat{\delta}_1 = \xi_{11}$$

$$\tan\hat{\delta}_j = \sum_{i=1}^{j}\sum_{i'=1}^{j} X_{ii'} \sin\xi_{ii'} / \sum_{i=1}^{j}\sum_{i'=1}^{j} X_{ii'} \cos\xi_{ii'}, \qquad j \geqslant 2 \tag{47}$$

$$\psi_1 = \phi_0$$

$$\psi_j = (\psi_1 + \hat{\delta}_{j-1}) - \text{Re } e^{i\psi_1} \sum_{j=1}^{j-1}\sum_{j''=j'}^{j-1} X_{j'j''} e^{i\xi_{j'j''}}. \tag{48}$$

R_j and T_j in Eqs. (39) to (47) are given for $j \geqslant 2$ by

$$R_j = \left[\frac{1}{\bar{k}_{z,j}} \tan(\bar{k}_{z,j}\bar{L}_j/2)(e^{i\Delta_0\bar{L}_j} + 1) - \frac{i}{\Delta_0}(e^{i\Delta_0\bar{L}_j} - 1)\right]\frac{1}{\Delta_0^2 - \bar{k}_{z,j}^2}, \tag{49}$$

$$T_j = \frac{1}{\bar{k}_{z,j}^2}\left[\frac{\bar{k}_{z,j}}{\Delta_0} \cdot \frac{\Delta_0\bar{L}_j \tan(\bar{k}_{z,j}\bar{L}_j/2) - i\bar{k}_{z,j}\bar{L}_j}{\Delta_0^2 - \bar{k}_{z,j}^2} - \frac{e^{i\Delta_0\bar{L}_j} - 1}{\Delta_0^2}\right.$$

$$\left. + i\,\frac{2e^{i\Delta_0\bar{L}_j/2}}{(\Delta_0^2 - \bar{k}_{z,j}^2)^2}\left\{(\Delta_0^2 + \bar{k}_{z,j}^2)\sin\frac{\Delta_0\bar{L}_j}{2} - 2\Delta_0\bar{k}_{z,j}\cos\frac{\Delta_0\bar{L}_j}{2}\tan\frac{\bar{k}_{z,j}\bar{L}_j}{2}\right\}\right]. \tag{50}$$

From Eqs. (39) and (48) the terms X_{ij} may be interpreted as generalized "bunching parameter." X_{jj} is the contribution from self-perturbations in the jth stage, and X_{ij} is the perturbation transmitted from ith stage of the amplifier.

The average change in γ at the end of the jth cavity $(\bar{z} = \sum_{i=1}^{j} \bar{z}_i + \bar{L}_i)$ is shown to be

$$<\frac{\Delta\gamma}{\gamma}> = -\frac{\bar{p}_{\perp 0}}{\gamma_0^2} \text{Re} \sum_{i=1}^{j} \bar{E}_{0i} R_i <e^{i\psi_i}>_{\phi_0} = -\frac{\bar{p}_{\perp 0}}{\gamma_0^2} \text{Im} \sum_{i=1}^{j} J_1(\hat{X}_{i-1}) \bar{E}_{0i} R_i. \tag{51}$$

The efficiency $\eta = -<\Delta\gamma>/(\gamma_0 - 1)$ in the jth cavity $(j \geqslant 2)$ can be calculated by taking the difference of $<\frac{\Delta\gamma}{\gamma}>$ between the $(j-1)$th and the jth cavity. Thus

$$\eta_j = \frac{\bar{p}_{\perp 0}}{\gamma_0(\gamma_0 - 1)} \text{Im } [J_1(\hat{X}_{j-1})\bar{E}_{0j}R_j]. \tag{52}$$

In Eqs. (51) and (52), $\text{Im}(x)$ denotes the imaginary part of x. The output power at the end of jth cavity is

$$P_{\text{out}} = \eta_j P_b, \tag{53}$$

where $P_b = V_b I_b$ is the beam power. The input signal power P_{IN} is given by

$$P_{\text{IN}} = \frac{\omega U_{mn}}{Q_1} - \eta_1 P_b, \tag{54}$$

where η_1 is the efficiency in the first cavity, and U_{mn} the stored energy in TE_{mn}^0 mode is

$$\omega U_{mn} = \frac{\pi\epsilon_0 m_0^2 c^5}{e^2} \bar{L}_1 \bar{r}_{w,1}^2 \bar{\omega}\left(1 - \frac{m^2}{x_{mn}^2}\right) J_m^2(x_{mn})$$

$$\cdot \frac{\beta_{\parallel}^2 \bar{E}_{01}^2}{J_{m-1}^2(\bar{k}_{mn}\bar{r}_0)} \cdot \left[\frac{\sinh 2\bar{k}_z^I \bar{L}_1}{2\bar{k}_z^I L_1} - \frac{\sin 2\bar{k}_z^R \bar{L}_1}{2\bar{k}_z^R \bar{L}_1}\right], \tag{55}$$

where k_z^R and k_z^I are the real and imaginary parts of $\bar{k}_{z,1}$. Since ϕ_0 is uniformly distributed in the range $0 \leqslant \phi_0 \leqslant 2\pi$, the average of $\Delta\gamma$ in the first cavity calculated from Eq. (34) vanishes. To calculate η_1, it is therefore necessary to expand $\frac{\Delta\gamma}{\gamma_0}$ in the first cavity to second order in E_{01}, and we obtain for $j = 1$

$$< \frac{\Delta\gamma}{\gamma} > = \frac{\bar{E}_{01}^2}{2\gamma_0^2}\left[|R_1|^2 + \frac{\bar{\Omega}_0^2\bar{p}_{\perp 0}^2}{\gamma_0^3\beta_\parallel}\,\mathrm{Im}S_1\right], \tag{56}$$

where

$$\begin{aligned} S_1 = {} & \frac{1}{\{\Delta_0^2 - \bar{k}_{z,1}^{*2}\}^2}\left[\Delta_0 k^*_{z,1}\bar{L}_1\left\{\frac{i(1-\cos 2k_{z,1}^R\bar{L}_1}{2\bar{k}_z^R\bar{L}_1} + \frac{1-\cosh 2k_z^I\bar{L}_1}{2k_z^I\bar{L}_1}\right.\right. \\ & + \left.\left.\frac{(\Delta_0^2 + \bar{k}_{z,1}^{*2})L_1}{2}\left\{\frac{\sinh 2\bar{k}_z^I L_1}{2\bar{k}_z^I L_1} - \frac{\sin \bar{k}_z^R\bar{L}_1}{2\bar{k}_z^R\bar{L}_1}\right\}\right]\right. \\ & - \frac{R_1}{(\Delta_0^2 - \bar{k}_{z,1}^{*2})^2}\cdot\left\{(\Delta_0^2 + \bar{k}_{z,1}^{*2})\sin \bar{k}_{z,1}^*\bar{L}_1 + 2i\Delta_0\bar{k}_{z,1}^*\cos \bar{k}_{z,1}^*\,\bar{L}_1\right\} \\ & - \frac{\bar{k}_z^*\cos \bar{k}_{z,1}^*\bar{L}_1 - i\Delta_0\sin \bar{k}_{z,1}^*\bar{L}_1}{(\Delta_0^2 - \bar{k}_{z,1}^{*2})}\left\{\frac{\sin \bar{k}_{z,1}\bar{L}_1 - \bar{k}_{z,1}\bar{L}_1 e^{i\Delta_0\bar{L}_1}}{\Delta_0^2 - \bar{k}_{z,1}^2} + \frac{2i\Delta_0 R_1}{\Delta_0^2 - \bar{k}_{z,1}^2}\right\}. \end{aligned}$$

The amplifier gain in dB is

$$g = 10\log_{10}\frac{P_{\mathrm{out}}}{P_{\mathrm{IN}}}. \tag{58}$$

In the small signal regime, both P_{out} and P_{IN} are proportional to E_{01}^2, and g becomes independent of P_{IN}. From Eqs. (53) and (57), it is clear that $P_{\mathrm{IN}} = 0$ and $g \to \infty$ when $\eta_1 P_b = \omega U_{mn}/Q_1$ with $\eta_1 > 0$. This corresponds to the self-oscillation of the input cavity.

If the beam has an axial velocity spread, then $\bar{E}_{0j}$ in equations for $\bar{p}$, X_{ij}, η, and $\frac{\Delta\gamma}{\gamma}$ should be replaced by $(\beta_{\parallel,av}/\beta_\parallel)\,\bar{E}_{0j}$. Furthermore, an average over the initial velocity distribution should also be performed to calculate the average values of $<p>$ and $<\frac{\Delta\gamma}{\gamma}>$. The expression for $\bar{E}_{0l}$ in Eq. (41) will also involve an average over the initial electron velocity distribution. In the expression for stored energy U_m in Eq. (46), $\beta_\parallel$ should be replaced by $\beta_{\parallel,av}$. The average over the initial distribution function is done numerically using a Gaussian distribution.

We have considered the interaction of the electron beam with the TE°_{mn} modes of circular waveguide. However, the results for TE°_{11} mode could be applied to the $TE^\square_{10}$ in the rectangular waveguide with the following substitution [10,11]:

$$\begin{array}{rcl} TE^\circ_{11} & & TE^\square_{10} \\ k_{11} = x_{11}/r_w & \to & \pi/L_x \\ c_{11}k_{11}J_0(k_{11}r_0) & \to & \sqrt{\dfrac{2}{L_xL_y}}\,J_0(\pi r_0/L_x) \\ J_1'(k_{11}r_0) & \to & J_1'(\pi r_0/L_x) \\ J_1(k_{11}r_0)/k_{11}r_0 & \to & J_1(\pi r_0/L_x)/(\pi r_0/L_x). \end{array}$$

L_x and L_y are lengths of the cavity along the x- and y-axis.

The small signal gain is calculated in the next section from Eqs. (52) to (58). The difference in phase between the output and the input signals can be obtained from the phase of the complex field amplitude $\bar{E}_{0j}$ (Eq. 41) assuming that E_{01} is real.

RESULTS AND DISCUSSION

In this section we calculate the small signal performance characteristics of a three-cavity gyroklystron amplifier [2] operating at the fundamental $TE^{\square}_{101}$ mode of rectangular cavity. The parameters of the cavities are: $L_1 = L_2 = 0.9\lambda_0$, $L_3 = 1.1\lambda_0$, $d_1 = d_2 = 1.5\lambda_0$, $r_0 = 0.136\lambda_0$, $Q_1 = Q_2 = 650$, and $Q_3 = 235$. L_x of the cavities are chosen to make the resonant frequency (f_0) of the cavities identical and $L_y/L_x = 0.9$. Results for a "cold" beam ($\Delta V_z/V_z = 0$) are shown in Figs. 2 to 6.

In Fig. 2 we show the variation of the small signal gain with the magnetic field for three values of beam current ($I_b = 1$, 3, and 6 A). The beam voltage V_b is 33.5 kV and $\alpha = v_\perp/v_\parallel = 1.0$. The frequency $f = 1.0016 f_0$. As shown in Fig. 1, amplifier operation is possible in different ranges of the magnetic field. For stable amplifier operation, the beam power, P_b, should be less than $P^{th}_{b,i}$ (the threshold beam power for onset of oscillations in cavities $i = 1, 2, 3$). In the case of $I_b = 6$A, gain occurs for the magnetic field lying in the ranges $5.7 < 2\pi \frac{\Omega_0}{\omega_0} < 5.95$ and $5.98 < \frac{2\pi\Omega_0}{\omega_0} < 6.3$. The gain as a function of the magnetic field shows resonance behavior at fields where the Doppler-shifted cyclotron frequency is equal to the operating frequency. The peak at $\bar{\Omega}_0 \cong 5.79$ corresponds to the condition $(\bar{\omega} - \bar{\Omega}_0/\gamma)L/v_\parallel = \pi$ for the first two cavities, and the peak at $\bar{\Omega}_0 \cong 5.95$ corresponds to this condition at the last cavity. Although the gain is high in this magnetic field range, a stable amplifier operation may not be possible since the gain is very sensitive to variations in the magnetic field. For magnetic field in the range $5.98 < \frac{2\pi\Omega_0}{\omega_0} < 6.3$, the gain is insenstitive to variations of magnetic field and $P_b < P^{th}_{b,i}$ ($i = 1, 2, 3$). Therefore, stable amplifier operation with relatively high gain is possible in this magnetic field range. In subsequent calculations, the parameters are optimized for maximum gain in the stable region of operation.

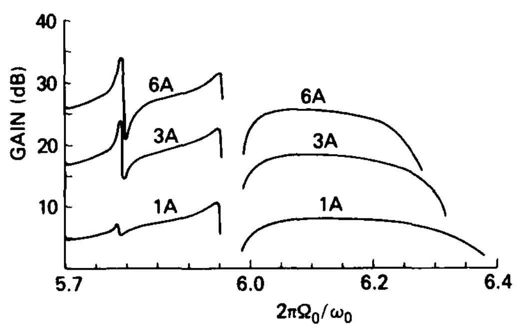

Fig. 2 — Small signal gain vs magnetic field for $I_b = 1$, 3, and 6 A. Other parameters are $V_b = 33.5$ kV, $\alpha = 1.0$, $f/f_0 = 1.0016$, $\Delta v_z/v_{z0} = 0.0$.

Figure 3 shows the small signal gain as a function of frequency for three values of $\alpha = v_\perp/v_\parallel = 1.0$, 1.5, and 2.0 with $V_b = 33$ kV and $I_b = 6$ A. The magnetic field is optimized for maximum gain (in the region of stable operation) at each α. The bandwidth at uniform magnetic field is extremely small (~0.2%). The gain increases and the bandwidth decreases as $v_\perp/v_\parallel$ is increased. The magnetic field needed for maximum gain also increases with $v_\perp/v_\parallel$ since $v_\parallel$

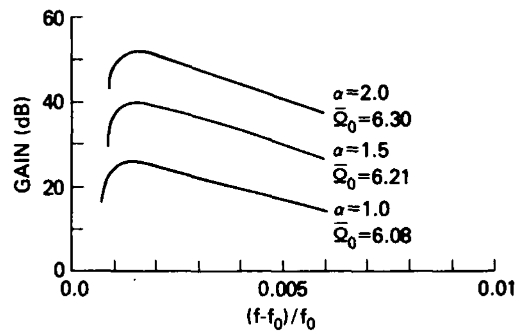

Fig. 3 — Gain as a function of frequency for three values of α = 1.0, 1.5, and 2.0 for I_b = 6 A. Other parameters are the same as in Fig. 2.

decreases. The frequency of maximum gain $f = 1.0016 f_0$ is insensitive to the change in α. The variation of gain with α is shown in Fig. 4 for $f = 1.0016 f_0$, $V_b = 33.$ kV, and $I_b = 6$ A. The magnetic field is optimized for maximum gain at each α. The corresponding magnetic fields are also shown in the figure. Initially, the gain increases linearly with α and then approaches saturation. The phase difference (ξ) between the input and the output signals is also calculated as a function of the various parameters such as beam voltage, current, magnetic field, drive power, and α. ξ is found to be a sensitive function of all these parameters except the current. In applications of gyroklystrons requiring precise phase control such as the RF linear accelerator, it is necessary to control these parameters very carefully. Figures 5 and 6 show the variation of ξ with V_b and $2\pi\Omega_0/\omega_0$.

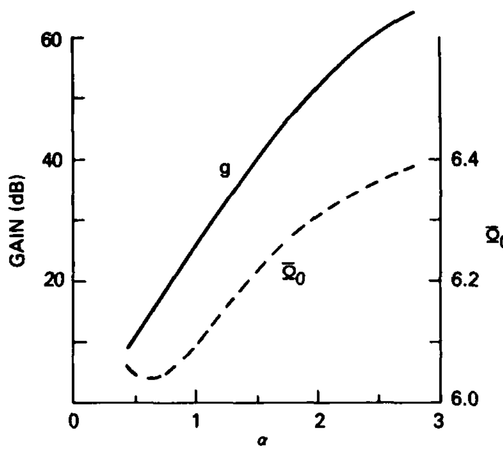

Fig. 4 — Plot of gain and the corresponding optimized magnetic field as functions of α. Other parameters are the same as in Fig. 2.

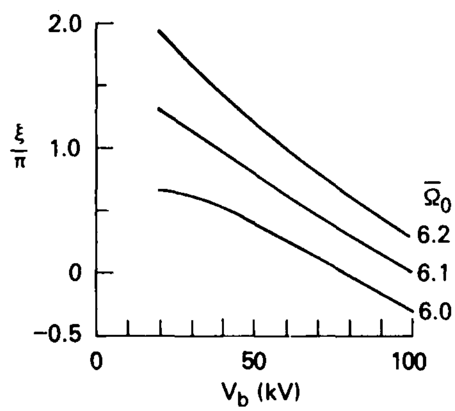

Fig. 5 — The variation of the phase difference (ξ) between the input and output signals as a function of beam voltage for three values of magnetic field. I_b = 4.0 A, α = 1.0, and f/f_0 = 1.0016.

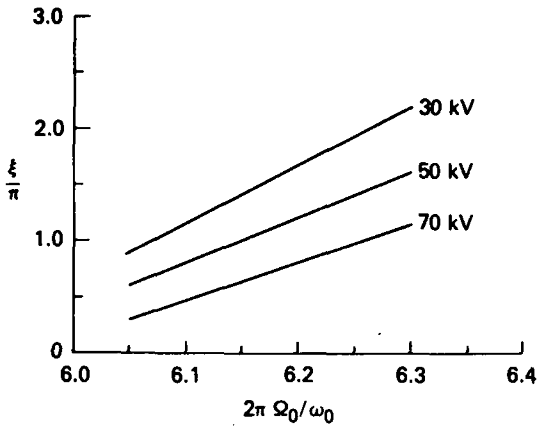

Fig. 6 — ξ as a function of the magnetic field for three values of V_b. Other parameters are the same as in Fig. 5.

Figures 7 and 8 show the effect of the axial beam velocity. A Gaussian velocity distribution function is assumed, i.e., $f(p_\perp, p_\parallel) \propto \exp\{(p_z - p_{z0})^2/2(\Delta p_z)^2\}\,\delta(p_\perp^2 + p_\parallel^2 - p_0^2)$. The gain and the corresponding optimized magnetic fields are shown as a function of $\Delta v_z/v_{z0}$ in Fig. 7. The gain decreases as $\Delta v_z/v_{z0}$ increaeses, and the magnetic field needed for optimum gain is also increased. The dependence of the small signal gain on the magnetic field is shown in Fig. 8 for several values of $\Delta v_z/v_{z0}$. As the beam velocity spread increases, there is not only a decrease in gain but the range of the magnetic field for stable amplifier operation also decreases rapidly. Stable operation of a gyroklystron amplifier for velocity spread $\Delta v_z/v_{z0} > 15\%$ will be difficult.

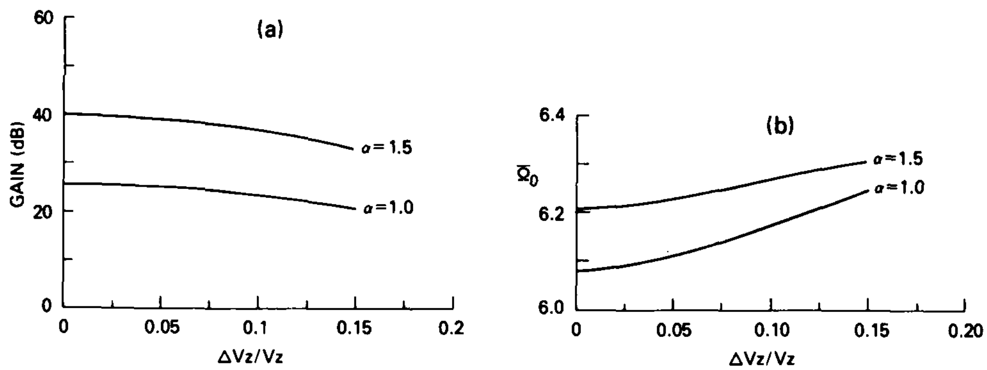

Fig. 7 — Maximum gain and the corresponding magnetic field as functions of $\Delta v_z/v_z$ for $\alpha = 1.0$ and 1.5. $V_b = 33.5$ kV, $I_b = 6$ A, and $f/f_0 = 1.0016$

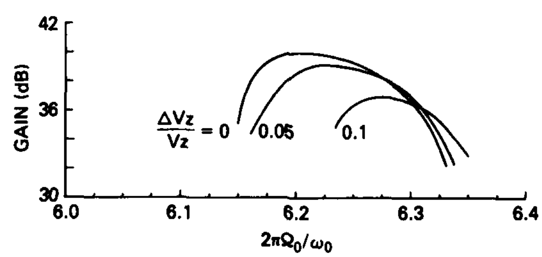

Fig. 8 — Gain vs magnetic field for different values $\Delta v_z/v_z = 0$, 0.05, and 0.10 at $\alpha = 1.0$. Other parameters are the same as in Fig. 7.

CONCLUSIONS

We have derived a comprehensive small signal theory of the multicavity gyroklystron. An analytic solution is obtained for the "cold" beam case. The use of the Green's function approach makes it possible to satisfy the boundary conditions for arbitary k_z (hence ω), and the gain as a function of frequency can be calculated. The stagger-tuned cavity configuration can also be investigated. The bandwidth in a uniform magnetic field is found to be very small. The bandwidth can be increased by using stagger-tuned cavities, but in a uniform magnetic field this leads to a reduction in gain. Caplan [7] has shown that the gain of the stagger-tuned cavity configuration is significantly increased by proper taper of the magnetic field. We plan to extend the present theory to include a nonuniform field. The present theory also represents the first iteration of a large-signal theory based on successive approximations. The small signal theory in the bunching cavities can be combined with a large signal theory in the output cavity to obtain a complete description of the multicavity gyroklystron amplifier. This theory should become a useful tool for obtaining design parameters of the multicavity gyroklystron.

ACKNOWLEDGMENTS

We are grateful to Drs. R. K. Parker, B. Arfin, and W. M. Bollen for many helpful discussions. The work is supported by ONR and NAVELEX.

REFERENCES

1. R. H. Jory, F. Friedlander, S. J. Hegji, J. F. Shively, and R. S. Symons, "Gyrotrons for High Power Millimeter Wave Generation," Intl. Elec. Dev. Meeting Tech. Digest, Washington, D.C., 1977, pp. 234-237.

2. W. M. Bollen, A. K. Ganguly, B. Arfin, C. Sedlak, and R. K. Parker, "Performance Characteristics of a Three-Cavity Gyroklystron," Tech. Digest, IEDM Conf. on Elec. Devices, San Francisco, Dec-9-12, 1984, pp. 838-840.

3. E. M. Demidovich, C. S. Kovalev, A. A. Kuryev, and F. G. Shevchenko, "Efficiency-Optimized Cascaded Circuits Utilizing the Cyclotron," *Radio Engy. Electron Physics* **18**, 1542-1549 (1973).

4. V. I. Kanavets and O. I. Klimov, "The Electron Efficiency of a Monotron and Klystron with a Relativistic Polyhelical Electron Beam," *Radio Engy. Electron Phys.* **21**, 78-83 (1976).

5. A. K. Ganguly and K. R. Chu, "Analysis of Two-Cavity Gyroklystron," *In. J. of Elec* **51**, 503-519 (1981).

6. R. S. Symons and H. R. Jory, "Small Signal Theory of Gyrotrons and Gyroklystrons," Proc. 7th Symp. Energy Problems of Fusion Research, Knoxville (*IEEE*, New York, 1977), pp. 1111-1115.

7. M. Caplan "Gain Characteristics of Stagger-Tuned Multicavity Gyroklystron Amplifier," Conf. digest of 8th Intl. Conf. on Infrared and mm Waves, Dec. 12-17, Miami Beach, Florida, paper W 4.2 (1983).

8. V. A. Flyagin, A. L. Goldenberg, and G. S. Nusinovich, "Powerful Gyrotrons" Infrared and Millimeter Waves, K.J. Button, ed., (Academic Press, New York, 1984) Vol. 11, pp. 179-226.

9. G. N. Rapoport, A. K. Nemak, and V. A. Zhurakhovskiy, "Interaction Between Helical Electron Beams and Strong Electromagnetic Cavity Fields at Cyclotron Harmonic Frequencies," *Radio Engineering and Electron Phys.* **12**, 587-595 (1967).

10. A. W. Fliflet, M. E. Read, K. R. Chy, and R. Seely, "A Self-Consistent Field Theory for Gyrotron Oscillators: Application to a Low *Q* Gyrotron," *Intl. J. Elec.* **53**, 505-521 (1982).

11. A. K. Ganguly and S. Y. Ahn, "Self-Consistent Large Signal Theory of Gyrotron Traveling Wave Amplifier," *Intl. J. of Elec.* **53**, 641-658 (1982).

END

FILMED

2-86

DTIC